Thermo-economic comparison of coal-fired boiler-based and groundwater-heat-pump based heating and cooling solution – A Case study on a greenhouse in Hubei, China

Jin Luo[a], Wei Xue[a], Haibing Shao[b]

[a]China University of Geosciences (Wuhan), Faculty of Engineering, Wuhan 430074, P.R. China

[b]Helmholtz-Zentrum für Umweltforschung, Leipzig, Sachsen, Germany

*Corresponding author: Jin Luo

Telephone: +8602767883044

Fax number: +8602767883507

Email address: jinluo@cug.edu.cn

Abstract:

Currently in China, the replacement of coal-fired boilers by clean and renewable energy sources is considered as an essential measure to alleviate air pollution. This paper investigates the thermo-economic performance of replacing a coal-fired boiler by a Groundwater Heat Pump (GWHP) system for a greenhouse, where the GWHP system was constructed to reduce emission and also to provide cooling. The operation of this system has been monitored over a one–year period. The results show that the thermal efficiency factor of the boiler varies in the range of 0.53-0.68 and the coefficient of performance (COP) of the GWHP system averages at 4.1 for cooling and at 3.3 for heating. Although the boiler has both lower capital costs and lower operating costs, the analysis of average energy price (AEP) shows that the GWHP system has a higher economic performance, since it has a lower AEP of 0.049-0.081 USD /kWh in heating and 0.029-0.061 USD/kWh in cooling, in comparison to the boiler at 0.053-0.084 USD/kWh. This shows that GWHP system may be cost

effective over traditional boilers for applications in other places of the world with similar climate condition.

Keywords: Greenhouse heating and cooling, Air-conditioning system, Boiler heating, Groundwater-heat-pump system, Thermo-economic performance

1 Introduction

In recent years, the high emission from coal burning and resulting air quality issues are attracting a lot of public attention in China [1]. Many strategies have been proposed or developed to alleviate its environmental impact. One of the effective solutions is to reduce the emission by switching the fossil-fuel based heating systems to a renewable energy based source [2]. Besides the environmental effects, thermo-economic performance is the key to the implementation and public acceptance of the transition [3]. Among all the emerging techniques, ground source heat pump (GSHP) system was considered to have high potential as a clean energy alternative to the conventional fossil-fuel system in space heating and cooling [4]. GSHP system delivers very high thermal efficiency by coupling the subsurface as the heat source in winter and heat sink in summer [5]. However, for large-scale greenhouses that imposes a high thermal demand, the capital costs of GSHP systems remains higher than that of the traditional boilers [6]. Thus, both thermal and economic performance should be carefully examined for a system replacement.

As a mature technology, the performance of boiler system is well investigated. Wang et al. conducted an economic analysis of a field monitored boiler heating system in New York State (NYS), USA [7]. The results indicated that the boiler system stays with different thermal efficiency and fuel price. It is thermo-economically possible to replace the oil heating by wood pellet heating with considering the seasonal efficiency of 75.8% and the fuel price at that time in NYS. Kattan and Ruble analyzed four different boilers for residential heating in Lebanon

[8]. Their results showed that the electric boiler system had the highest polluting and lowest cost-effective system over its lifetime. In Comparison, olive husks, liquefied petroleum gas and diesel-powered boiler systems stay at nearly equal average energy prices that is lower than the electric boiler over the lifetime. The coal-fired boiler was populated and widely used for heating due to its easy installation and operation [9]. Boiler thermal efficiency varied widely between 0.6 and 0.8 by different designs of combustion chamber and system exergy [10, 11]. On the other side, it has been identified that the coal-fired boilers contribute significantly to air pollution and CO_2 emission [12].

On the clean energy side, the groundwater heat pump (GWHP) system is a type of GSHP systems with both high thermal and economic performance [13, 14]. Boon et al. implemented an experimental investigation on the open-loop GWHP system [15]. The Seasonal Performance Factor (SPF) was measured of 4.5 during the monitoring period. The changes in ground temperature vary between 2°C and 4°C at different seasons. It was indicated that the aquifers hold a huge potential for the city's heating and cooling demand by using the GWHP system. Zhen et al. investigated a solar-assisted GWHP system for the heating system of an airport in Tibet, China [16]. Thermal performance analyses showed that the coefficient of performance (COP) is about 5.0, which is much higher in comparison to conventional heating technologies in this region. It is well recognized that the availability of groundwater and subsurface permeability have significant impacts on the circulating flow rate, which in turn affect the efficiency of heat transfer of the GWHP systems [17]. An aquifer with high porosity and hydraulic conductivity was expected to have a high potential for GWHP installation [18]. From the above studies, it is also known that the thermo-economic performance of a boiler system related closely to the capital costs, thermal efficiency and fuel prices. In general, a boiler system stay rather low capital costs and the operating costs were sensitive to the price of fuel [19]. Compared to a boiler system, the GWHP system can commonly achieve higher thermal performance, but also higher capital costs [20]. Therefore, the system installation, system operation and thermal efficiency should be considered in order to achieve a successful transition from a boiler to a GWHP based system.

In the context of emission reduction, this case study focuses on a greenhouse in Zhongxiang county of Hubei province, China. There the original coal-fired boiler was replaced by a GWHP system in 2017. This study aims at examining the installation and operation of both systems to understand the performance difference and its origin. A thermo-economic comparison is made for both the boiler and the GWHP system. The manuscript is organized as follows. In section 2, the geological setting and the climatic conditions of the study area are characterized. In addition, the components and configuration of both systems are introduced, followed by the monitoring setup of the system the examination of its thermal performance. The economic performance of the system operation was assessed by considering the capital costs, operating costs and covered thermal loads of both systems in section 3. Lastly, the conclusions of this study are made in section 4.

2 Materials and study methodology

2.1 Geological background and system configuration

2.1.1 Geological setting and the climatic condition

The studied greenhouse is located in Zhongxiang city in the middle of China, as shown in Fig. 1. It is about 178 km west to the provincial capital Wuhan city. The greenhouse is situated on a river alluvial plain with good potential for agricultural development [21]. This area has a subtropical monsoon climate with a mean annual air temperature of 17.8°C and humidity of 77%. The recorded highest temperature is 39.7°C and the lowest temperature is -10.3°C. The monthly climatic data of the study area were presented in Table 1. Heavy rainfalls were mainly distributed from March till August. The wind speed remains rather stable, ranging from 2.5 m/s to 3.6 m/s. The study area stays a rather humid environment with humidity over 70% throughout the whole year. The air temperature indicates a rather hot summer and a cold winter, implying both heating and cooling are required to maintain a relatively stable temperature in the greenhouse.

2.1.2 Geological investigation

To characterize the subsurface conditions for the installation of production and injection wells of the GWHP system, geological investigations were carried out in the vicinity of the greenhouse. The drilling task was first conducted to determine the geological stratum of the site. A geological profile was then created by the borehole log. The hydraulic unit was also identified by the analysis of the collected drilling cores and cuttings. Thermal, physical and hydraulic parameters were measured either by laboratory or field tests.

- **Borehole log**: The drilling was implemented from the ground surface to the bedrock. River deposits were detected by analysis of the drilling cuttings. The collected drilling cuttings which contain majorly two categories of clay/silt and cobble. It is expected to have a high hydraulic conductivity of the cobble layer which could be treated as a potential aquifer. The geological profile of the site was summarized based on the drilling log. The subsurface down to 33.7 m depth was comprised of three layers: the upper clay/silt, the middle gravels and the bed rock, as shown in Fig. 2.

- **Thermo-physical properties of drilling cuttings:** Thermal parameters such as thermal conductivity, thermal diffusivity and thermal capacity are measured using a portable instrument ISOMET 2114. A needle probe was deployed in the soil measurements, as shown in Fig. 3(a). The soil samples were collected and prepared in a cylindrically shaped container with a 6 cm diameter and 11 cm height. The measuring accuracy of thermal conductivity is ±5.0% by calibrating the probe with reference materials. Besides, particle size distribution (PSD) of these drilling cuttings was determined by sieve analysis, as shown in Fig. 3(b). The soil samples were dried in an oven with a temperature of 55℃ over 24 h before the sieve analysis.

- **Pumping test:** In order to obtain the hydraulic parameters of the aquifers, in-situ pump tests were conducted. In the study area, the cobble layer was considered to be the potential confined aquifer and the water was mainly pumped out from this layer. A pumping well was drilled with a 300 mm diameter and until a depth of 28.6 m. An observation well was installed 6 m away from the pumping well, as shown in Fig. 4 (a). The amount of drawdown in the steady-state was determined during the pumping test and the hydraulic parameter was interpreted by following equation.

$$W = \frac{2\pi KD(s_w - s_1)}{\ln\left(\frac{r_1}{r_w}\right)} \quad (1)$$

where W is the pumping rate (m^3/s), KD is Transmissivity (m^2/s), s_w and s_1 are the respective water levels in the piezometers (pumping well and observation well), r_1 is the distance between pumping well and observation well (m), r_w is the radius of the pumping well (m) [23]. In addition, the water temperature was measured during the tests and the water samples were collected for later analysis of the PH value, electric conductivity and concentration of Fe^{2+}, Mn^{2+}, Ca^{2+}, Mg^{2+} cations, which contribute mainly the mineral precipitation, as shown in Fig. 4 (b).

2.1.3 System configuration

Fig. 5 presents an overview of the greenhouse and some of the drilling wells surrounded. It shows that the greenhouse consists of six individual sections with a total area of 17.54×10^4 m^2. Before 2017, this greenhouse was heated by a boiler which is located at the south-west corner as shown in Fig. 5. It was later replaced with a GWHP system under the pressure of reducing air pollution at the end of 2017. The

GWHP system was configured in the west boundary of the greenhouse. There are 30 pumping wells drilled around the greenhouse, with an average depth of 30 m and an adjacent distance of 60 m. Similarly, there are 30 recharging wells drilled with an adjacent distance of 50 m.

Fig. 6 shows the system configuration of the boiler heating system and the GWHP system. Briefly, the boiler system is comprised of a combustion chamber, water tanker, dust collector and a chimney, as shown in Fig. 6 (a). The GWHP system consists of the production/injection well, heat pump units and fan/radiators, as shown in Fig. 6(b). The GWHP is an open-loop system that pumps the groundwater from the wells marked in blue color and reinject it into wells highlighted in yellow color. In addition, four locations are selected randomly to monitor the temperature variation inside the greenhouse.

Table 2 lists the main components and their specifications of both the boiler and GWHP systems. The boiler system consists of 2 combustion chambers, 2 dust collectors, 2 blower fans, 2 draught fans and 2 water circulation pumps. The GWHP system was configured with 3 heat pumps, 18 desanders, 3 water circulation pumps to the greenhouse and 3 circulation pumps to the wells. The heat pumps have a total heating capacity of 3, 779 kW and a total cooling capacity of 3, 706 kW. The technical specifications of these components are listed in Table 2.

Fig. 7 displays the major components configured in both the boiler and GWHP systems. The water tank of the boiler system lay above the combustion chamber, as shown in Fig. 7(a). The combustion chamber was connected to the dust collector by pipes. Most of the dust was stored in the dust collector and the waste gas was emitted through the chimney. For the GWHP system, three heat pumps are parallel connected and linked to the wells via water pipes. The groundwater was pumped flowing through the heat pumps by the water circulation pumps to achieve heat extraction or dissipation, as shown in Fig. 7(b). All the wells are parallel connected through a manifold to a main pipe and the numbers of the operating wells were controlled by valves to meet the actual demand of the groundwater.

Fig. 8(a) shows an inside view of the greenhouse which was used for flower planting. To maintain a stable indoor temperature, fans and heat radiators were equipped in the system to provide air-conditioning (see Fig. 8(b) and Fig. 8(c)). The fans were configured with a layout of 8 m×16 m and the heat radiators pipe were parallelly lined with a 4 m distance. The boiler system was only operated for heating by the combustion of coal to provide the hot water. Thermal energy of the hot water was dissipated to the greenhouse by the radiators and fans. The GWHP system was used to provide both heating and cooling. In heating mode, the groundwater was pumped from the well and circulated through the heat pump. Thermal energy was extracted from the groundwater and the temperature of heat carrier fluid to the greenhouse was lifted to 40-45℃ by the heat pumps. In cooling mode, the heat carrier fluid from greenhouse was chilled down to 8-10℃ by the heat pump and then circulated back to the greenhouse. The waste heat was transferred to the groundwater and re-injected back into the subsurface.

2.2 Measurement setup

2.2.1 The meteorological conditions

The meteorological parameters including the air temperature and humidity have significant impacts on the thermal capacity of the greenhouse and the planning of GWHP systems. Rainfall and wind speed will greatly influence the ambient temperature and heat dissipation of the greenhouse. Thus, four climatic parameters including air temperature, humidity, rainfall and wind speed were continuously monitored with a one-hour interval in 2018.

2.2.2 Operation of the boiler

The boiler system was operated only for heating in winter. During the daytime, the greenhouse was heated directly by solar radiation and the boiler system started to operate from 17:00 till 7:00 the next day. The coal consumed by the boiler heating was recorded for each month in the winter of 2016/2017. Simultaneously, the fluid temperature and flow rate to the greenhouse were also monitored with a time interval of 1 h to estimate the thermal loads of the greenhouse.

2.2.3 Groundwater heat pump system

The operation of the GWHP was similar to the boiler system. It started at 17:00 PM and stopped by 7:00 AM the next day. Their difference is that the GWHP runs for both heating in summer and cooling in summer. Table 3 shows the parameters monitored during the GWHP system operation. For the greenhouse cooling, the system was monitored from June 26th, 2018 till August 16th, 2018. The heating period of the system was monitored from Oct 19th, 2018 till April 6th, 2019. More specifically, the monitoring setup including the temperature, fluid flow rate and power input of the GWHP system operation was listed in Table 3.

2.3 Thermal performance analysis

The thermal performance of the GWHP is estimated by considering the parameter of the coefficient of performance (COP) for heating or energy efficiency ratio for system cooling. COP/EER is an essential indicator that represents the thermal efficiency of a system with considering energy input and output. Briefly, COP of a system can be given as:

$$\mathrm{COP/EER} = \frac{Q}{N} \quad (2)$$

where COP is the coefficient of performance for heating (-), EER is the system performance for cooling (-), Q is the heating/cooling capacity (kWh) of the system, N

is the energy input for running a system (kWh).

In the present work, the energy output for both the boiler and GWHP system is the heating or cooling capacity of the greenhouse. Energy inputs for the boiler differ from that of the GWHP system. For the boiler system, the coal consumed and electricity input for operating the water-circulating pumps to the greenhouse are considered. For the GWHP system, all the electricity input for operating the heat pumps, water circulation pumps to wells and to greenhouses are considered. The detailed definition of the COP for these two types of systems is shown as:

$$\eta_{boiler} = \frac{Q}{M \times q} \times 100\% \tag{3}$$

$$COP_{gwhp} = \frac{Q}{\sum N_i + \sum N_j} \tag{4}$$

$$Q = \sum_{i=1}^{n} \frac{V_i \rho_i c_i \Delta T_i}{3600} \Delta t_i \tag{5}$$

where η_{boiler} is the efficiency factor of the boiler (-), M is the daily coal consumption (kg/d) and q is the coal heating value (q=29.31MJ/kg). COP_{gwhp} is the heat pump system coefficient of performance (-), Q is the system capacity (kWh), $\sum N_i$ is all power consumed by heat pump unit (kWh), $\sum N_j$ is all power consumption of water circulation pumps (kWh), V_i is average fluid flow of user side in time i (m^3/h), Δt_i is is the heat pump operation at time i. V is heat pump unit user side average fluid flow (m^3/h), ΔT_i is the inlet and outlet fluid temperature difference from/to the greenhouse (℃), ρ is average density of water (kg/m^3), c is average heat capacity of water (kJ/(kg·℃)) [7, 24].

2.4 The economic performance

2.4.1 Capital costs

The capital costs of an air-conditioning system consist of the investment of components and the installation cost. For a boiler system, the components are comprised mainly of the combustion chamber, water tanks, dust collector and chimney, as shown in Table 2. A GWHP is rather complicated due to the drilling and installation of the pumping/recharging wells. Briefly, the capital costs of both boiler and GWHP systems can be formulated as:

$$C_{cap\_B} = \sum_{i=1}^{n} P_{com,i} \times N_i + C_{in} \quad (6)$$

$$C_{cap\_G} = \sum_{i=1}^{n} P_{com,i} \times N_i + \sum_{j=1}^{n} P_{drilling} \times N_j \times L_j \quad (7)$$

where C_{cap_B} is capital cost of the boiler heating system (USD), $P_{com,i}$ is price of the component (USD), N_i is the component i, C_{in} is installation fee (USD), C_{cap_G} is the capital costs of the groundwater heat pump system (USD), $P_{drilling}$ is drilling price per meter depth (USD/m), N_j is the drilling well j, L_j is the length of drilling well j (m) [25].

2.4.2 Operating costs

The main operating costs of the boiler system are the coal consumption and the electrical power input for running the dust removal and water-circulating pumps, as given in Eq. (8). On the other hand, the operating costs of the GWHP system were majorly comprised of the power input for production/injection water of the drilling wells, heat pump operation and water circulation pumps to the greenhouse, which is given as Eq. (9).

$$C_{\mathrm{oper\_B}} = Q_{e,B} \times P_e + Q_t \times P_{coal} + C_{main} \quad (8)$$

$$C_{\mathrm{oper\_G}} = Q_{e,G} \times P_e + C_{main} \quad (9)$$

where C_{oper_B} is the operating costs of the boiler system (USD/yr), $Q_{e,B}$ is electricity consumption by boiler system (kWh/yr), Q_t is coal consumed by boiler (t/yr), $Q_{e,G}$ is groundwater heat pump power consumption (kWh/yr), C_{oper_G} is the operation cost of the groundwater heat pump system (USD/yr), C_{main} is equipment maintenance (USD/yr), P_e is the electricity price (USD/kWh), P_{coal} is the coal price (USD/ton) [26, 27].

2.4.3 Analysis of economic performance

The economic performance of both the boiler and GWHP systems was examined by considering the capital costs and operating costs, and thermal load of the greenhouse. An average energy price, AEP, that represents the ratio of invests to the thermal load of a system was considered. It is an important indicator for the evaluation of the economic profitability of an investment. Smaller values indicate higher economic performances. The AEP can also be used for to compare different technical alternatives to determine which has the highest potential for a limited investment fund [19]. The AEP can be simply formulated as follows:

$$\mathrm{AEP} = \frac{C_{inv}}{Q_s} \tag{10}$$

$$C_{inv} = \begin{cases} C_{cap} + C_{ope} \times t & (\;for\ Boiler) \\ C_{cap} \times \frac{Q_{s,heating}}{Q_s} + T_{ope,\,heating} \times d \times t & (for\ GWHP\ heating) \\ C_{cap} \times \frac{Q_{s,cooling}}{Q_s} + T_{ope,\,cooling} \times d \times t & (for\ GWHP\ cooling\ ) \end{cases} \tag{11}$$

where C_{inv} is the energy price invested for both the system installation and operation (USD), Q_s is the thermal capacity of the system (kWh). T_{ope} is the daily operating costs ($T_{ope,\,heating} = 3,811\ USD/day$, $T_{ope,cooling} = 2,447\ USD/day$), d is the operating duration (d). All related costs used in the equation were set according to their values in 2019.

3 Results and discussion

3.1 Geological setting and climatic conditions

3.1.1 Geological and hydraulic conditions

The upper clay/silt layers have a total thickness of around 20 m and the middle cobble layer varies from 8 m to 10 m thickness in the study area. In terms of the hydraulic property, the cobble layer can be treated as an aquifer. Below and above this layer are the impermeable clay and claystone. Thus, the cobble layer is considered to be a confined aquifer. Particle size distribution (PSD) analysis was made and the coefficient of uniformity was determined of C_u=2.9 for the silt and C_u=5.7 for Cobble. It indicates that the Cobble layer has high uniformity, meaning a high hydraulic permeability.

Table 4 shows some of the recorded drawdown values obtained in the pumping tests. The undisturbed groundwater table is 3.0 m beneath the ground surface. The pumping tests were repeated three times. The pumping rate, hydraulic heads for both the pumping well and observation well were recorded for the interpretation of the hydraulic parameters by following Eq. (1). The results listed in Table 4 indicate that the aquifer with a mean hydraulic conductivity of 1.03×10^{-3} m/s, meaning a quite high potential for water production and injection. In addition, the temperature of the water pumped out of the drilling well was measured to be 17.0±0.5℃.

Table 5 presents the groundwater analysis of the water samples collected from the aquifers by pumping. It shows that the PH value is 7.09, implying suitable water for the GWHP application [28]. The ion analysis show that the Fe^{2+} is 0.84 mg/L, Ca^{2+} is 68.5 mg/L and Mg^{2+} is 20.3 mg/L for the collected water samples. These ions are important to estimate the mineral precipitation and pipe corrosion problems for the GWHP application. All these ion concentrations are detected with the threshold of the local standards [29]. In addition, the electric conductivity was 973 μS/cm which is smaller than the proposed lowest value causing pipe corrosion [24].

3.1.2 Climatic conditions

Fig. 9 shows the local climatic data including temperature, humidity, daily rainfall and wind speed in 2018. The temperature fluctuates dramatically over the year. In winter, the lowest temperature drops below the freezing point in December or January. The summer is rather hot with the maximum temperature constantly exceeding 35 ℃ from July till September, as shown in Fig. 9(a). The study area remains a rather humid environment with a mean humidity value of 80% through the year, as it is depicted in Fig. 9(b). The rain season lasts from April till September, as it is illustrated in Fig. 9(c), indicating a high groundwater table that has high potential for groundwater pumping. The rest periods are generally lower rainfall, which leads to low a groundwater table and a high potential for water injection into the ground. The daily wind speed is rather low in this area, ranging between 2.1 m/s and 3.4 m/s, as it is displayed in Fig. 9(d).

3.2 Thermal performance analysis

3.2.1 Boiler heating system

The heating efficiency of the boiler system was determined by considering coal consumed, power input and energy gain by the greenhouse. The monitoring data shows that the consumption of coal varies drastically with months in the heating period, as shown in Table 6. December in 2016 and January in 2017 consume 3, 332 tons coal which is more than half of the used coal of 5, 342 tons for boiler heating. Besides, the thermal energy converted by the coal combustion was also calculated to estimate the boiler efficiency by following Eq. (3).

The boiler efficiency factor was determined for the system operation from October 16^{th}, 2016 till April 17^{th}, 2017, as it is displayed in Fig. 10. The monthly values show that the efficiency factors of boiler changes between 53.28% and 68.05%, with a mean value of 60.61%. It illustrates that the boiler system stays rather low thermal efficiency by comparing it with the values reported in the literature [30, 31]. It implies high coal consumption for greenhouse heating, as it is verified in Table 6.

3.2.2 Thermal efficiency of the groundwater heat pump system

In the present work, the GWHP system was applied for both heating and cooling of the greenhouse, as the operation records presented in Table 7. In order to estimate the thermal performance of the GWHP system, the temperature of the fluid pumped from and back into the wells was monitored, as shown in Fig. 11(a). In the cooling case, the outlet temperature of the wells stays lower than the inlet temperature, indicating heat dissipation into the ground aquifers. The outlet temperature remains stable during the operation, whereas the inlet temperature fluctuates. Their difference varies between 4.1°C and 10.3°C with a mean of 7.9°C, indicating very high efficiency. In heating, the well outlet temperature expresses higher values that the well inlet temperature, implying a heat extraction by the heat pumps. The difference between inlet and outlet is round 4.3°C which is much lower than the cooling case, as it is illustrated in Fig. 11(b). This indicate that the system cooling performs higher efficiency that the heating.

The well outlet temperature was measured at the outlet of the wells and it therefore can represent the aquifer temperature. The initial aquifer temperature was measured of 17.5°C at June 26th, 2018 and gradually increased up to 18.5°C on August 16th, 2018 in the heating case. It implies that the temperature in aquifers was affected by the GWHP operation. The water stored in the aquifers was warmed up by the heat, as the high well inlet temperature shown in Fig. 11 (a), dissipated from the greenhouse. Thus, the increasing of well outlet temperature was detected in heating. On the contrary, in the cooling case, the well outlet temperature was dropping over time, as shown in Fig. 11 (b). The heat was extracted from water pumped out of the aquifers, resulting in temperature decreasing. The chilled water was later recharged into the aquifer which in turn reduces the aquifer temperature gradually with time.

Similarly, the fluid temperature circulates into and out of the greenhouse was also monitored. Both fluid inlet and out temperature fluctuate drastically in the cooling period, as shown in Fig. 12(a). A lower inlet temperature to the greenhouse than the outlet fluid temperature is observed, indicating a system cooling. On the other hand, the inlet temperature is higher than the outlet temperature in heating, as shown in Fig. 12(b).

In summer, the temperature inside the greenhouse fluctuates between 21℃ and 35℃ for system cooling at four monitoring points. The greenhouse needs to be cooled down from a high temperature to a low temperature, as shown in Fig. 13(a). It shows that the temperature peak drops rapidly to a certain low temperature, indicating a high efficiency in system cooling. In the system heating, the temperature inside the greenhouse shows a smaller temperature range around 3.5℃ difference, as shown in Fig. 13(b). This implies a more stable thermal performance of the greenhouse in the system heating.

The system thermal efficiency was estimated following Eq. (2) and Eq. (4). Fig. 14 illustrates the COP/EER values for the GWHP system in both heating and cooling cases. It shows that the EER for system cooling fluctuates between 2.5 and 5.6, with a mean value of 4.1, as shown in Fig. 14(a). The COP values vary from 2.4 to 5.8 with a mean value of 3.3, as it is depicted in Fig. 14(b), indicating the system heating is relatively lower thermal efficiency than that of cooling. Through the whole heating and cooling seasons, the GWHP system shows a similar thermal performance if compared against other GWHP systems installed in this area [32].

3.3 Comparison of the economic performance

3.3.1 Comparison of the capital cost and operating costs

The capital costs are essential to determine the economic performance of an energy system. Table 8 lists the individual component, number and price for both the system. The total capital costs were then determined by the sums of the entire component investment and the installation cost. It is accounted that the capital costs of the GWHP system are 716, 859 USD which is about 49.1% higher than that of the boiler system of 480, 423 USD

In this work, the operating costs represent the coal or electricity inputs to run the air-conditioning system to meet the energy demand of the greenhouse. Thus, the power consumption such as coal used and electricity input for the operation of the system was considered of the boiler system. For the GWHP system, electricity input for running the heat pumps and water circulation pumps was taken into account. The operating costs over one year were determined and the results are presented in Table 9. The operating cost of the GWHP system is about 694, 202 USD which is slightly higher than the boiler system which has an annual operating cost of 769, 437 USD. This could be attributed to the longer operating duration of the GWHP system, as it is verified in Table 7.

3.3.2 The system economic performance

The system investments were assessed by referring to the capital costs in section 3.3.1 and the annual operating costs. The average daily temperature, the highest and lowest temperature monitored by over 30-year period was applied to determine the heating and cooling duration, as shown in Fig. 15. In the present work, the 70 days cooling and 165 days for heating were determined by considering the highest temperature over 30°C in summer and the lowest temperature less than 12.5°C in winter. Table 10 illustrates the estimated annual operating costs of both the boiler and the GWHP system. The GWHP system has relatively higher annual operating costs of 800, 232 USD than that of the boiler system which is 677, 771 USD. Thus, the system investments of the GWHP system are higher than the boiler system by considering both capital and operating costs.

Moreover, the thermal loads of the greenhouse were estimated by considering the seasonal COP/EER and the annual operating period. The results show that the GWHP system covers 20.46 million kWh and the boiler is 13.75 million kWh annually, as shown in Table 10. The higher thermal load of the GWHP system than the boiler can be attributed to the GWHP was used for serving the greenhouse cooling in summer.

The above studies show that the GWHP system has higher capital costs and also higher operating costs as compared to the boiler system. It shows that the annual investments of the boiler is lower than the GWHP system and their difference keeps enlarging, as shown in Fig. 16(a). Note that the GWHP was not only operated for heating, but also for cooling. The GWHP investments were separated here into heating and cooling parts. It shows that each the heating or cooling investments are lower than that of the boiler system. On the other hand, the annual thermal capacity for the boiler and GWHP systems are also plotted in Fig. 16(b). The covered thermal load of the greenhouse by GWHP system is higher than the boiler system due to the same heating load and the additional GWHP cooling.

To compare the economic performance, the AEP of both systems is examined for heating and cooling, separately. It illustrates that the AEP of both systems starting with a rapid decreasing and tends to be steadily trending with time. The AEP of GWHP was lower than the boiler system in the estimated operation period, as it is illustrated in Fig. 17. The AEP values of the boiler system drop from 0.084 USD/kWh down to 0.053 USD/kWh for heating. For the GWHP system, the AEP decreases from 0.081 USD/kWh till 0.049 USD/kWh for heating, and drop from 0.061 USD/kWh till 0.029 USD/kWh for cooling. Their relatively difference becomes larger and larger from 3.7% up to 8.2%. The results indicate higher economic performance of the GWHP system for both heating and cooling. Thus, a successful system replacement to a conventional coal-fired boiler system was achieved by the GWHP system in term of the thermo-economic performance.

In this particular case, one of the major reasons for the success of the GWHP system replacement attributes to the shallowly bedded aquifers and high hydraulic conductivity, as it is verified in the geological investigation. The very shallow bedded aquifer with high hydraulic conductivity leads to low capital costs and a high potential for groundwater pumping. Thus, to make a successful GWHP system installation, the site geological conditions deserve to be carefully characterized [33]. On the other hand, the air pollution caused by the emission of the coal-fired boiler can be effectively alleviated by deploying the GWHP system. Although the GWHP system has higher installation and operation costs, the average energy price is lower. Moreover, the system cooling made by the GWHP brings further economic profits by extending the production period of the greenhouse for two more months than boiler system annually.

4 Conclusions

This paper investigates thermo-economic performance of the air-conditioning system of a greenhouse which was renovated from a coal-fired boiler to the GWHP system. To estimate thermal performance, system operation was monitored over a one-year period for each system. Then, the capital costs and operating costs of both systems are evaluated. The economic performance of both systems is examined by considering the system investments and the covered thermal load of the greenhouse. The major findings obtained from this study are made:

- Geological setting and the feasibility of GWHP installation: The study area is a typical subtropical climate area that has a hot summer and a rather cold winter. It is, therefore, heating and cooling energy is both demanded by the air-conditioning of a greenhouse. However, the formerly installed boiler system cannot service for cooling, resulting in a system shut down in summer. Moreover, air pollution caused by the coal-fired boiler calls for imperatively shutting down by the local government. By considering the above concerns, the air-conditioning system has to be switched to a system with high thermal performance and environmental friendliness. GWHP system is a considerable alternative due to the high thermal efficiency and emission free. The geological investigation shows the ground was a river deposited area with high potential for groundwater pumping. A mean hydraulic conductivity is 1.03×10^{-3} m/s of the aquifer is determined by a field pumping test, indicating a very high potential for GWHP installation. Thus, it is highly feasible to replace the boiler to a GWHP system.

- Thermal performance analysis: The GWHP system was installed in 2017 to replace the former boiler system which was constructed in early 2016. In order to estimate thermal performance of these systems, system operation for the boiler system during October 2016 till April 2017 and the GWHP system from June 2018 till April 2018 were monitored. The thermal efficiency of the boiler is estimated varies between 0.53 and 0.68, and the COP of the GWHP system expresses a higher COP/EER values of 3.3 for heating and 4.1 for cooling. The thermal advantages of the GWHP system are remarkable due to the high COP values for both heating and cooling. Furthermore, the GWHP system used in summer for the greenhouse cooling brings additional benefits for the flower production.
- Economic performance: The assessment of economic performance was made by taken into account the capital costs, operating costs and thermal load of the greenhouse. The results show that the GWHP has both higher capital costs and operating costs than the boiler system. Meanwhile, the GWHP system achieves a higher thermal load by the summer cooling. To evaluate the economic performance, the average energy price (AEP), which represents the economic performance was assessed over a 10-year period. It shows that the AEP of both systems keeps steadily decreasing annually, from 0.084 USD/kWh to 0.053 USD/kWh of the coal-fired boiler. It decreases from 0.081 USD/kWh to 0.049 USD/kWh in heating and drop from 0.061 USD/kWh to 0.029 USD/kWh in cooling of the GWHP system. Thereby, the AEP of the GWHP was lower than that of the coal-fired boiler system, indicating a higher economic performance.

Acknowledgements

This work was financially funded by the National Natural Science Foundation of China (NSFC) (authorized No. 41877200). The authors would thank also the Fundamental Research Funds for the Central Universities, China University of Geosciences (Wuhan) CUGL150818 and CUGL180407.

References

[1] Chen JM, Li CL, Ristovski Z, Milic A, Gu YT, Islam MS, Wang SX, Hao JM, Zhang HF, He CR, Guo H, Fu HB, Miljevic B, Morawska L, Thai P, Lam YF, Pereira G, Ding AJ Huang X, Dumka UC. A review of biomass burning: Emissions and impacts on air quality,health and climate in China. Science of the Total Environment 2017; 579: 1000-1034.

[2] Zhang QL, Hao YY, Sun DH, Nie Q, Jin LW. Research on the Clean Energy Heating Systems in Rural Beijing. Energy Procedia 2017; 143: 137-143.

[3] Yilmaz F. Energy, exergy and economic analyses of a novel hybrid ocean thermal energy conversion system for clean power production. Energy Conversion and Management 2019; 196: 557-566.

[4] Wu SY, Dai YC, Li XL, Oppong F, Xu CS. A review of ground-source heat pump systems with heat pipes for energy efficiency in buildings. Energy Procedia, 2018: 152: 413-418.

[5] Li WX, Li XD, Wang Y, Tu JY. An integrated predictive model of the long-term performance of ground source heat pump (GSHP) systems. Energy and Buildings 2018; 159:309–318.

[6] Cui YL, Zhu J, Twaha S, Chu J, Bai HY, Huang K, Chen XJ, Zoras S, Soleimani Z. Techno-economic assessment of the horizontal geothermal heat pump systems: A comprehensive review. Energy Conversion and Management 2019; 191: 208-236.

[7] Wang K, Zhang Y, Sekelj G, Hopke PK. Economic analysis of a field monitored residential wood pellet boiler heating system in New York State. Renewable Energy 2019; 133: 500-11.

[8] Kattan P, Ruble I. An economic assessment of four different boilers for residential heating in Lebanon. Energy and Buildings 2012; 50: 282-289.
[9] Liu SC, Li Z , Dai BM. Energy, Economic and Environmental Analyses of the CO2 Heat Pump System Compared with Boiler Heating System in China. Energy Procedia 2017; 105: 3895-3902.
[10] Wang DJ, Liu LS, Yuan Y, Yang H, Zhou YX, Duan RZ. Design and key heating power parameters of a newly-developed household biomass briquette heating boiler. Renewable Energy 2020; 147: 1371-1379.
[11] Zhang Q, Yi HN, Yu ZH, Gao JT, Wang XZ, Lin HY, Shen B. Energy-exergy analysis and energy efficiency improvement of coal-fired industrial boilers based on thermal test data. Applied Thermal Engineering 2018; 144: 614–627.
[12] Han YF, Shen B, Zhang T. A Techno-economic Assessment of Fuel Switching Options of Addressing Environmental Challenges of Coal-Fired Industrial Boilers: An analytical work for China. Energy Procedia 2017; 142: 3083-3087.
[13] Aresti L, Christodoulides P, Florides G. A review of the design aspects of ground heat exchangers. Renewable and Sustainable Energy Reviews 2018; 92: 757-773.
[14] Noorollahi Y, Saeidi R, Mohammadi M, Amiri A, Hosseinzadeh M. The effects of ground heat exchanger parameters changes on geothermal heat pump performance – A review. Applied Thermal Engineering 2018; 129: 1645-1658.
[15] Boon DP, Farr GJ, Abesser C, Patton AM, James DR, Schofield DI, Tucker DG. Groundwater heat pump feasibility in shallow urban aquifers: Experience from Cardiff, UK. Science of The Total Environment 2019; 697: 133847.
[16] Zhen JL, Lu J, Huang GQ, Zhang HY. Groundwater source heat pump application in the heating system of Tibet Plateau airport. Energy and Buildings 2017; 136: 33-42.
[17] Zhou XZ, Gao Q, Chen XL, Yu M, Zhao XW. Numerically simulating the thermal behaviors in groundwater wells of groundwater heat pump. Energy 2013; 61: 240-247.
[18] Wang GL, Wang WL, Luo J, Zhang YH. Assessment of three types of shallow geothermal resources and ground-source heat-pump applications in provincial

capitals in the Yangtze River Basin, China. Renewable and Sustainable Energy Reviews 2019; 111: 392-421.
[19] Kattan P, Ruble I. An economic assessment of four different boilers for residential in Lebanon. Energy and Buildings 2012; 50: 282-289.
[20] Lu Q, Narsilio GA, Aditya GR, Johnston I W. Economic analysis of vertical ground source heat pump systems in Melbourne. Energy 2017; 125: 107-117.
[21] Dong W, Wu TJ, Luo JC, Sun YW, Xia LG. Land parcel-based digital soil mapping of soil nutrient properties in an alluvial-diluvia plain agricultural area in China. Geoderma 2019; 340: 234-248.
[22] China National Meteorological Information Center. Daily data set of ground accumulated annual value in China (1981-2010). 2019 http://data.cma.cn/data/.
[23] Birsoy YK, Summers WK. Determination of aquifer parameters from step tests and intermittent pumping data. Ground Water 1980; 18:137-46.
[24] GB/T 50801-2013, Evaluation standard for application of renewable energy in buildings, China Architecture & Building Press, Beijing, China 2013.
[25] Zheng TY, Shao HB, Schelenz S, Hein P, Vienken T, Pang Z. Kolditz O, Nagel T. Efficiency and economic analysis of utilizing latent heat from groundwater freezing in the context of borehole heat exchanger coupled ground source heat pump systems. Applied Thermal Engineering 2016; 16: 314-326.
[26] Bălănescu DT, Homutescu VM. Experimental investigation on performance of a condensing boiler and economic evaluation in real operating conditions. Applied Thermal Engineering 2018; 143: 48-58.
[27] Hadi FA, Fujii H, Hiroyuki K. Cooling tests, numerical modeling and economic analysis of semi-open loop ground source heat pump system. Geothermics 2018; 71: 34-45.
[28] GB 50019-2003, Code for design of heating ventilation and air conditioning, China Architecture & Building Press, Beijing, China 2004.
[29] Bai XL, Cheng KH. Key factors of water quality affecting fouling of the river water source pump heat exchanger. Journal of Water Resources & Water Engineering 2013; 23: 44-47.

[30] Gu H, Zhu HX, Cui YF, Si FQ, Xue R, Xi H, Zhang JY. Optimized scheme in coal-fired boiler combustion based on information entropy and modified K-prototypes algorithm. Results in Physics 2018; 9: 1262-1274.

[31] Ma L, Fang QY, Yin CG, Zhong L, Zhang C, Chen G. More efficient and environmentally friendly combustion of low-rank coal in a down-fired boiler by a simple but effective optimization of staged-air windbox. Fuel Processing Technology 2019; 194: 106-118.

[32] Luo J, Luo ZQ, Xie JH, Xia DS, Huang W, Shao HB, Xiang W, Rohn J. Investigation of shallow geothermal potentials for different types of ground source heat pump systems (GSHP) of Wuhan city in China. Renewable Energy 2018; 118: 230-244.

[33] Birks D, Coutts CA, Younger PL, Parkin G. Development of a groundwater heating and cooling scheme in a Permo-Triassic sandstone aquifer in South-West England and approach to managing risks. Geoscience in south West England 2015; 13: 428-436.

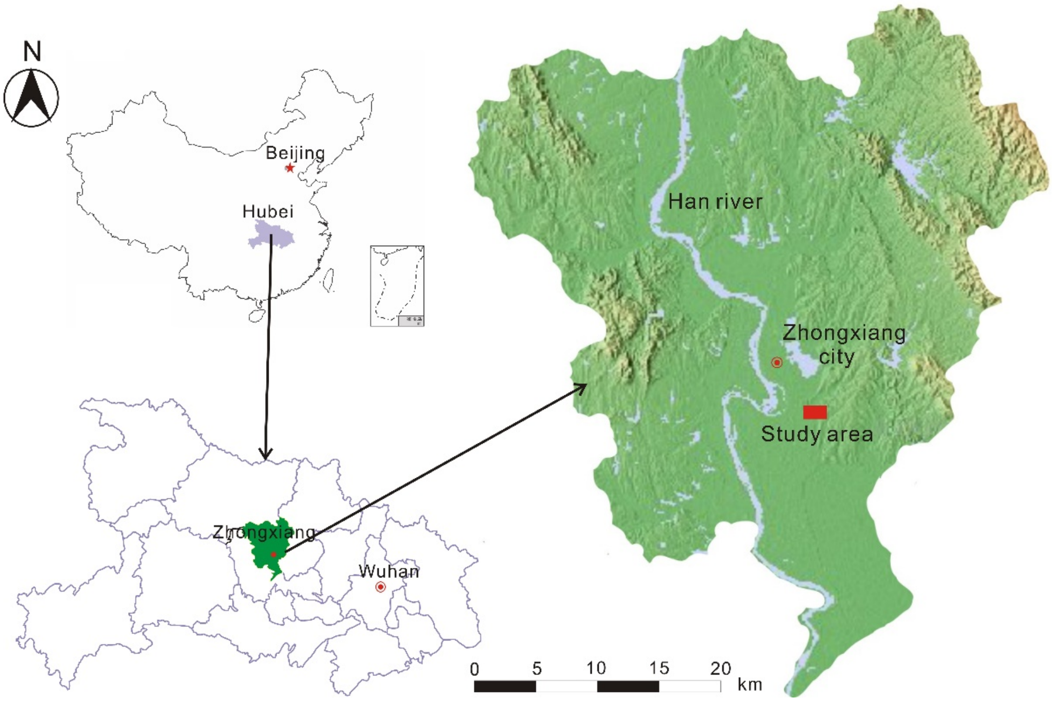

Fig. 1 The location of the greenhouse in Zhongxiang city of Hubei province in China

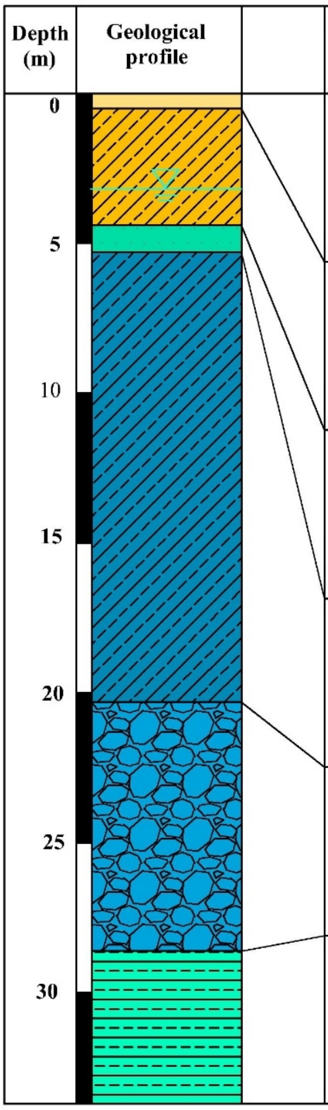

Geological age	Thickness (m)	Lithology	Thermal conductivity (W/m·K)	Specific heat capacity (kJ/kg·K)	Thermal diffusivity (mm^2/s)
Q_4^{pd}	0.50	Cultivated soil	—	—	—
Q_4^{al}	3.90	Silty clay	1.19	1.43	0.59
Q_4^{al}	0.90	Silt	1.62	1.89	0.86
Q_4^{al}	15.00	Silty clay	1.13	1.30	0.87
Q_4^{al+pl}	8.30	Cobble	1.55	1.39	1.12
K	5.10	Sandstone	5.46	2.85	1.92

Fig. 2 The geological profile logged at the construction site of the greenhouse

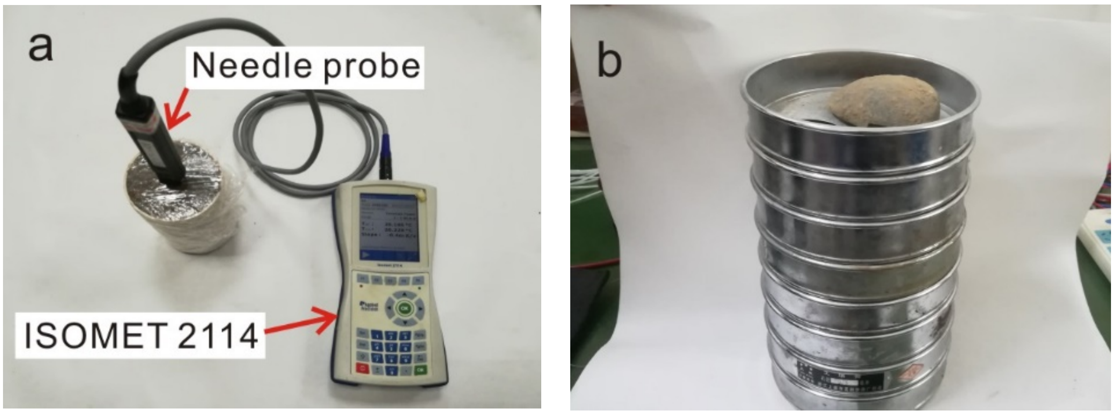

Fig. 3 The determination of thermo-physical property of the drilling cuttings (a. Thermal properties measurements of the soil sample, b. particle size distribution (PSD) analysis of the samples)

a. Pumping test for hydraulic parameters b. Analysis of the groundwater sample

Fig. 4 The wellhead of the pumping well and water sample analysis at the greenhouse in Zhongxiang city Hubei province of China

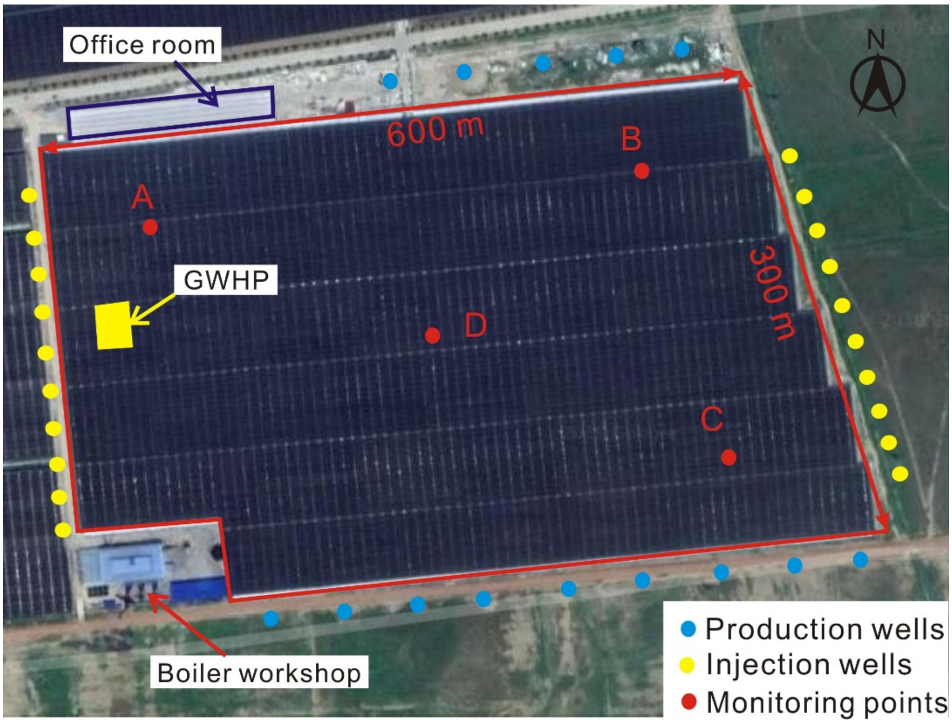

Fig. 5 Location of the boiler and GWHP system with respect to the greenhouse

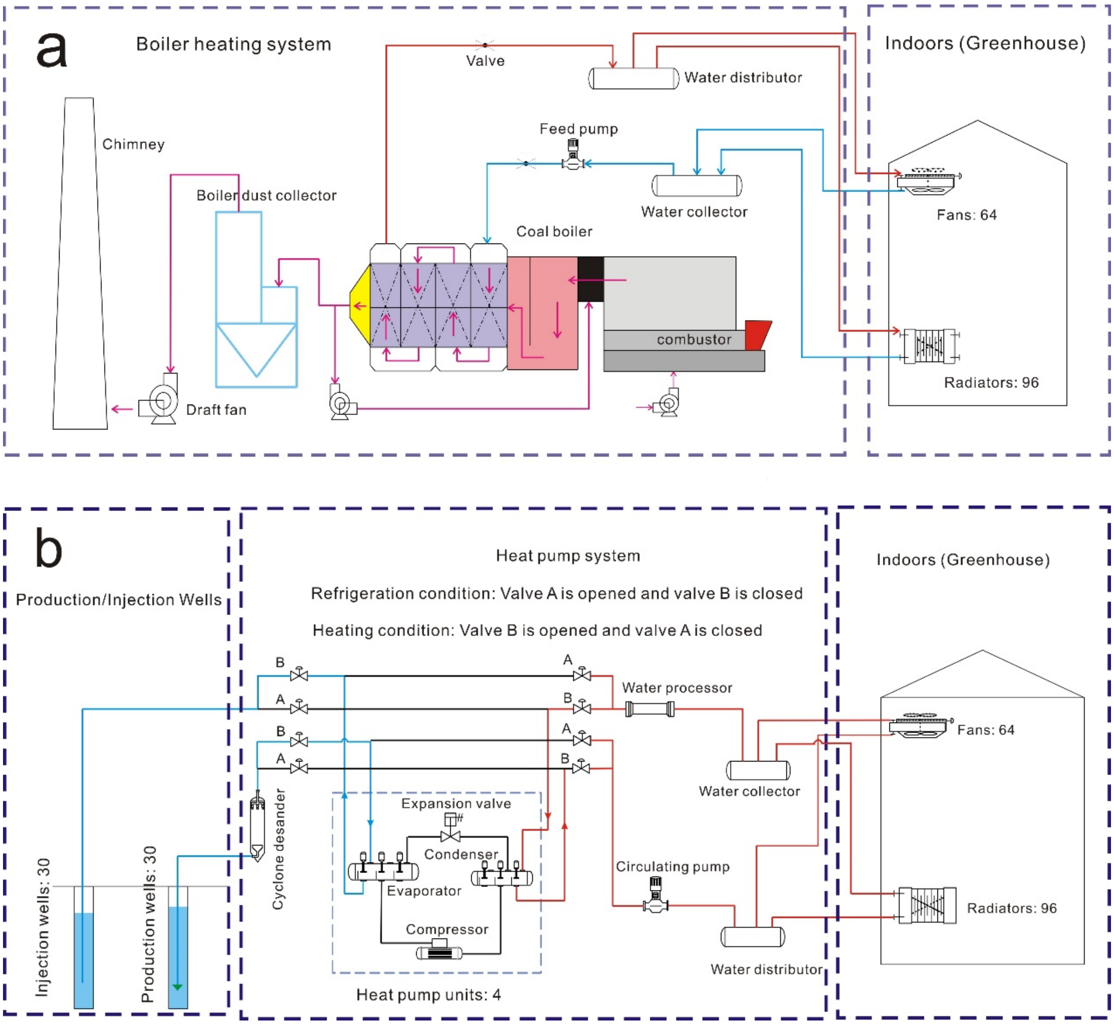

Fig. 6 The schematic diagram shows that the air conditioning system of the greenhouse replaced from boiler heating to GWHP (a. The boiler heating system, b. The GWHP system)

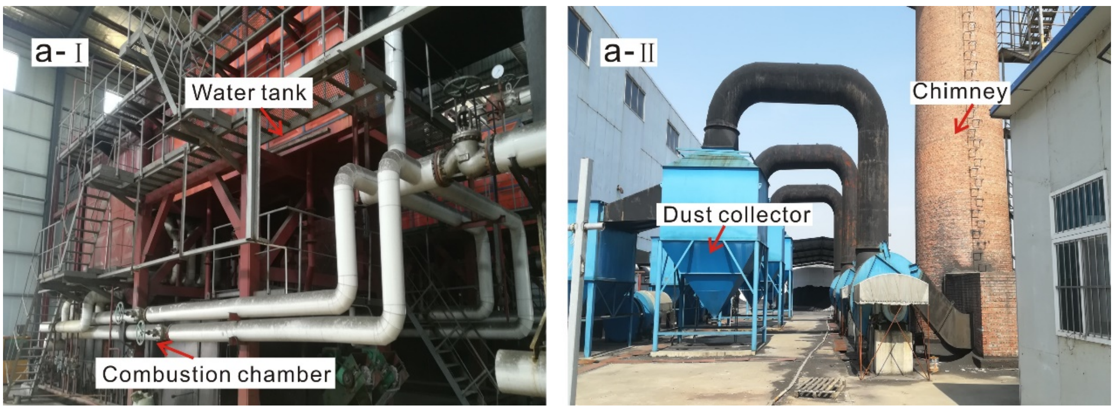

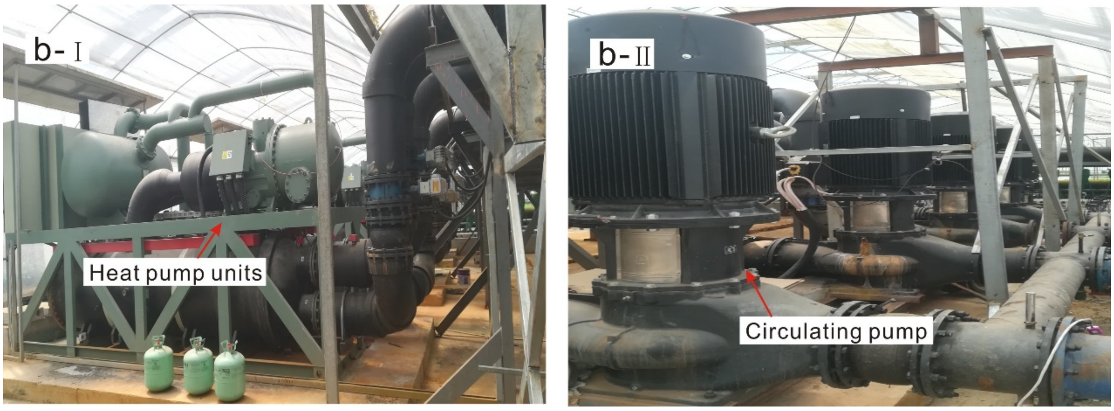

Fig. 7 Components of both the boiler and GWHP systems (a. The boiler system: a_I is the water tanks and coal combustion chamber, a_II is the dust collector and chimney; b. The groundwater heat pump system: b_I is the heat pumps, b_II is the water circulation pumps)

Fig. 8 Air-conditioning components configured inside the greenhouse (a. An overview inside the greenhouse, b. Fans and c. Heat radiator)

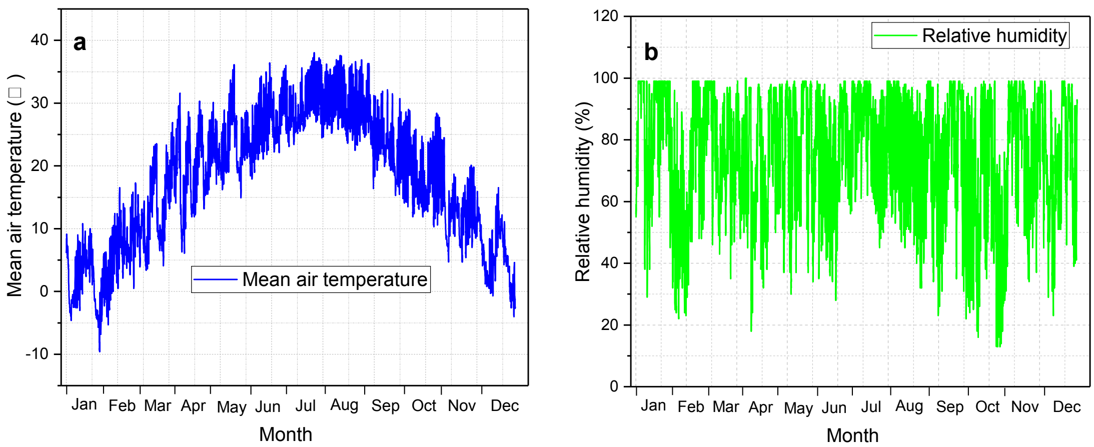

(a) Temperature variation in 2018 (b) Humidity

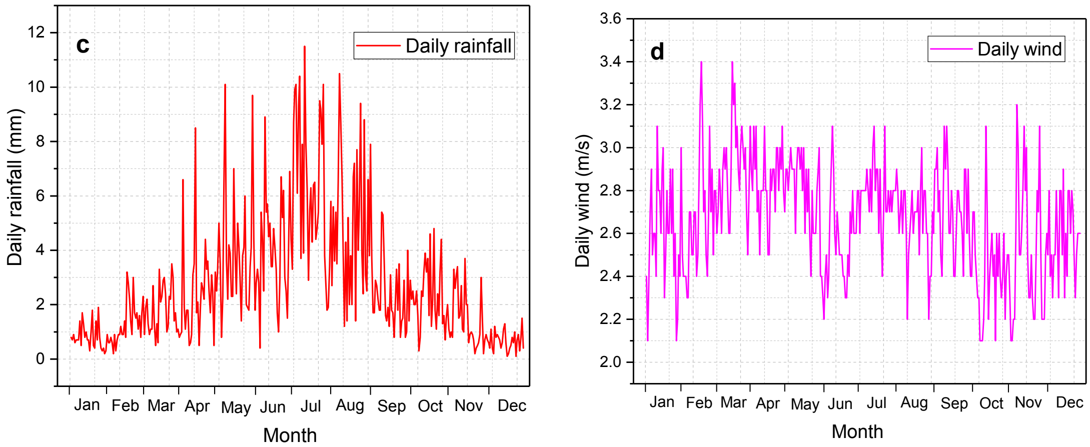

(c) Rainfall (d) Wind speed

Fig. 9 The monitored hourly temperature, humidity, rainfall and wind speed of Zhongxiang city between 0:00 on January 1st, 2018 and 23:00 December 31th, 2018

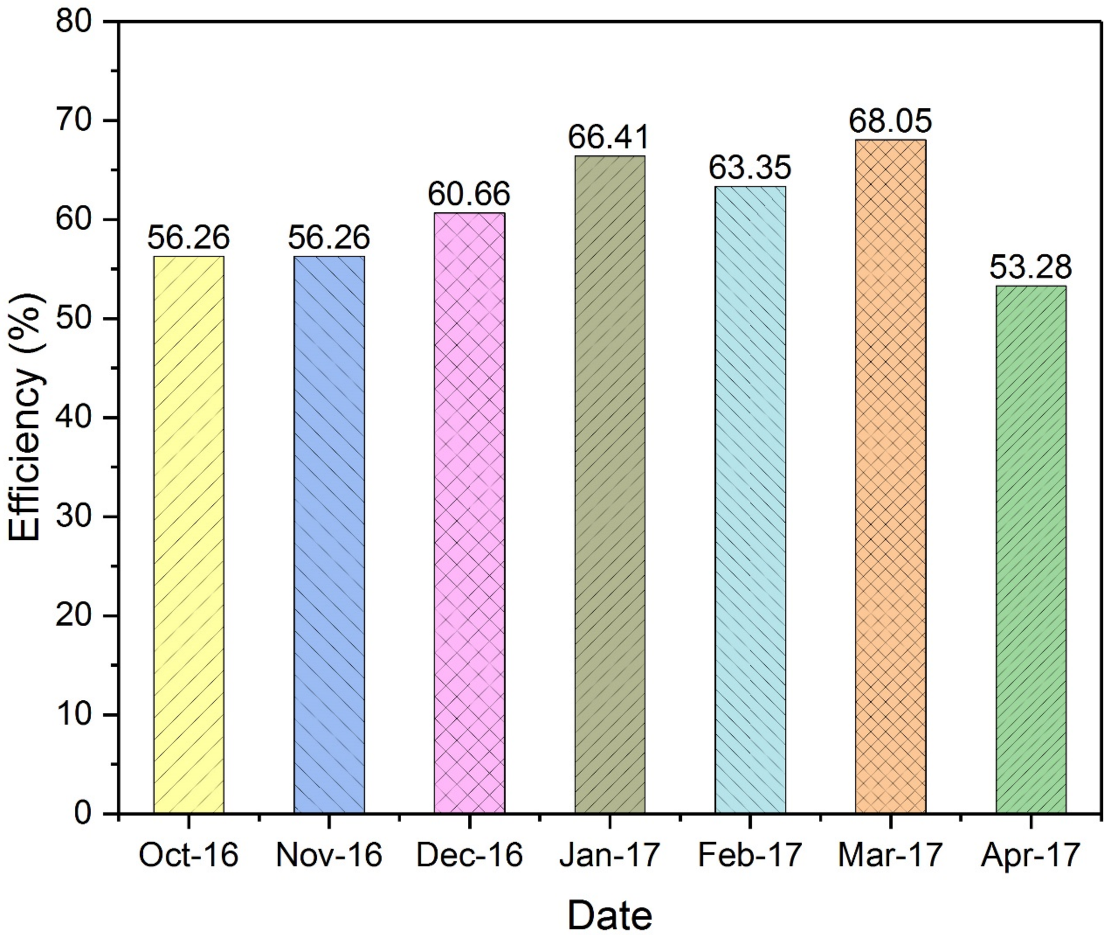

Fig. 10 The variation of the boiler efficiency from October 2016 till April 2017

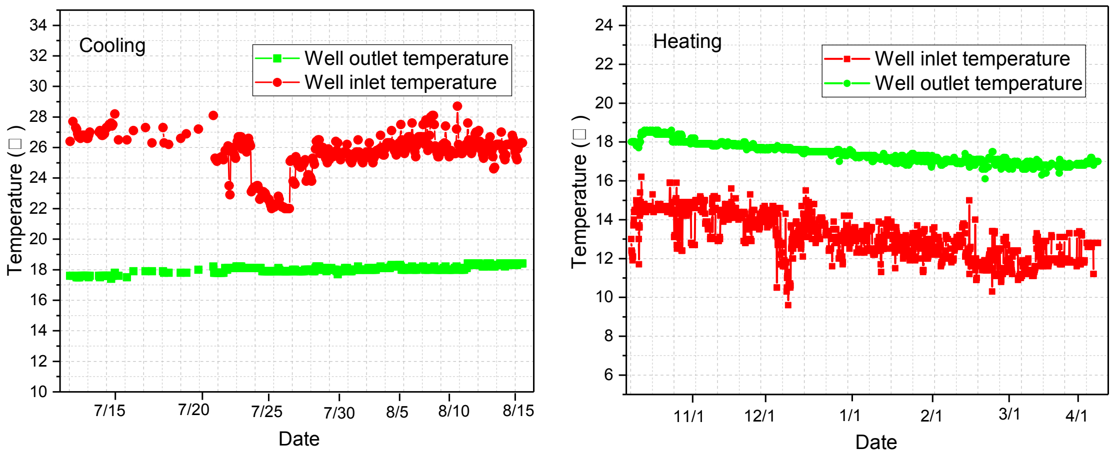

(a) Fluid inlet and outlet temperature to the pumping well in cooling

(b) Fluid inlet and outlet temperature to the pumping well in heating

Fig. 11 The monitored fluid temperature of the water pumping from and recharging into the wells

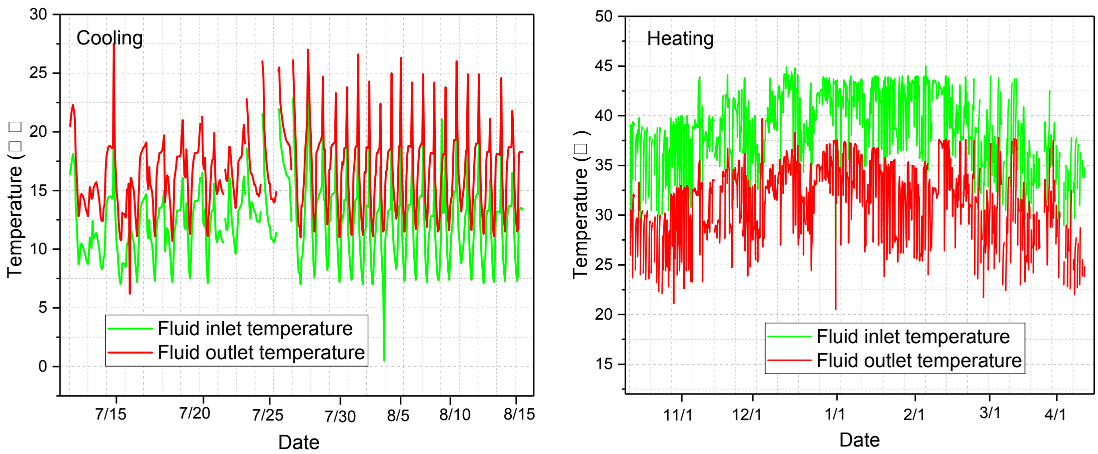

(a) The recording of the fluid inlet and outlet temperature of the greenhouse in cooling

(b) The recording of the fluid inlet and outlet temperature of the greenhouse in heating

Fig. 12 Inlet and outlet fluid temperature circulates into the greenhouse and flows back from the greenhouse

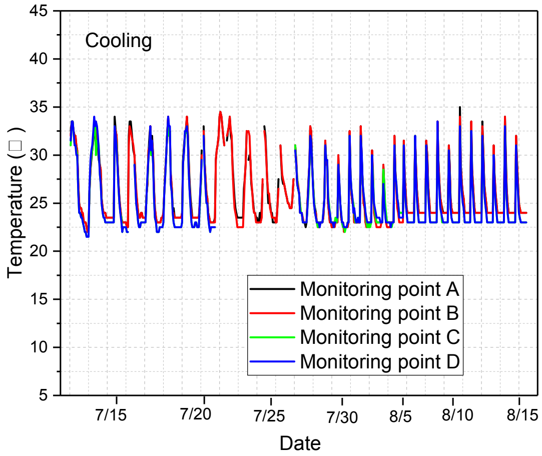

(a) The temperature inside the greenhouse in summer at four monitoring points

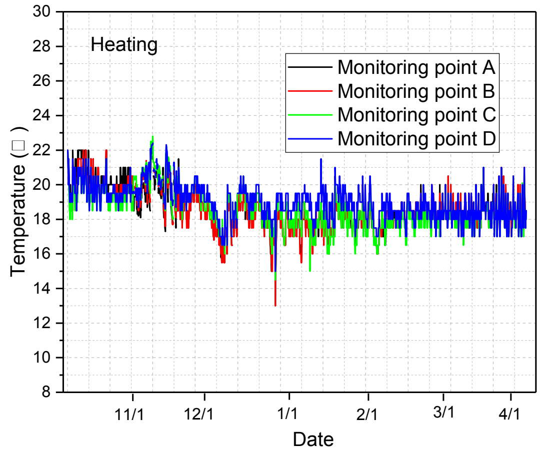

(b) The temperature inside the greenhouse in winter at four monitoring points

Fig. 13 The recorded indoor temperature of the greenhouse at four different points

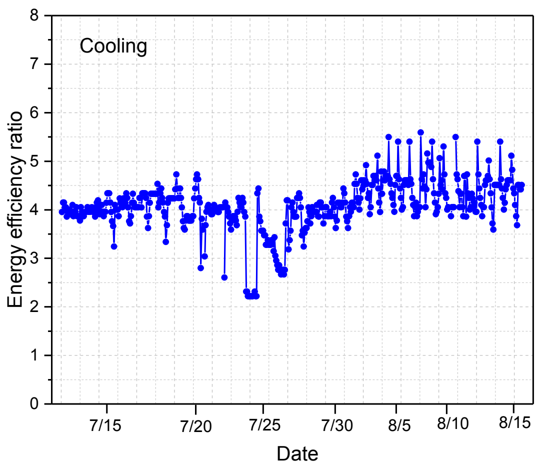

(a) The estimated cooling performance of the GWHP system

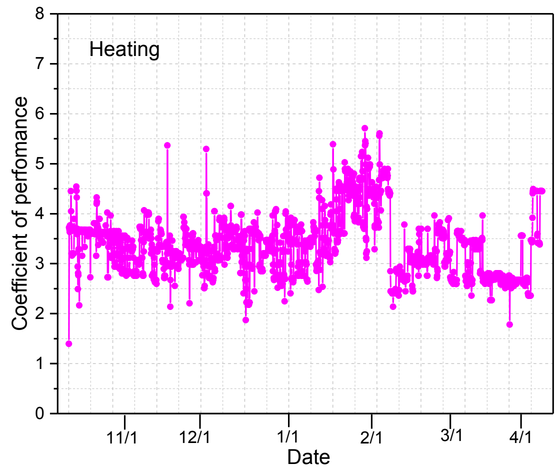

(b) The estimated heating performance of the GWHP system

Fig. 14 The estimated thermal performance of both the heat pump systems and groundwater heat pump system

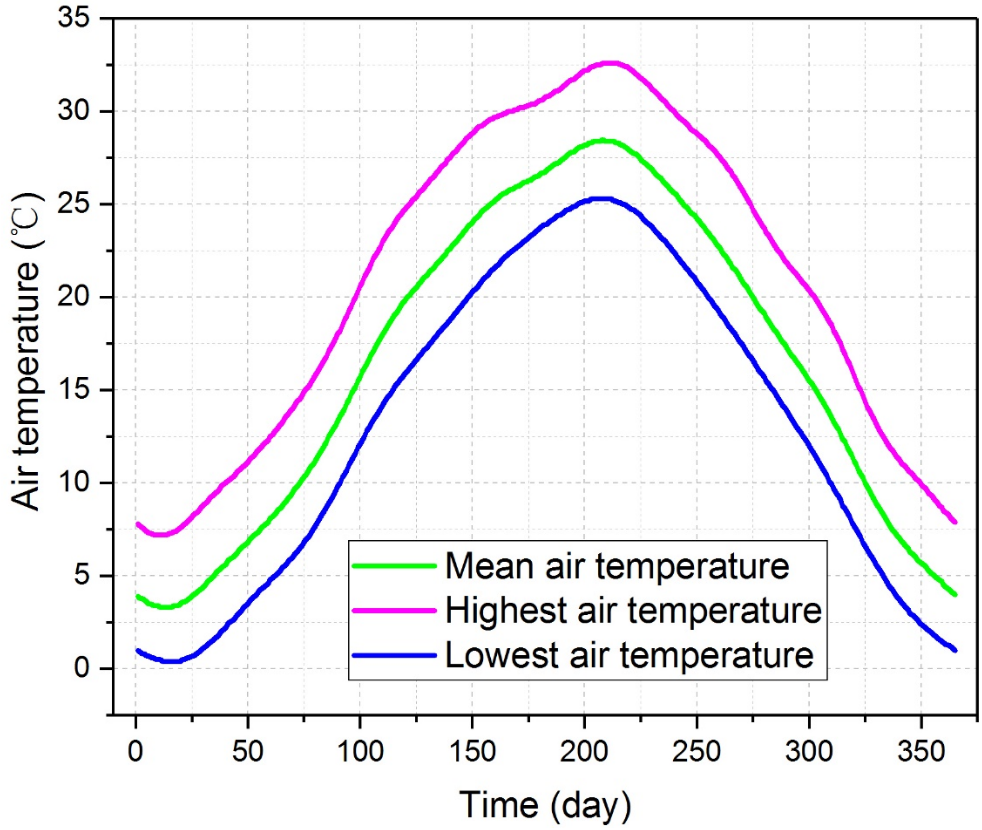

Fig. 15 The daily temperature from 1981 to 2010 in Zhongxiang county of Hubei province, China [22]

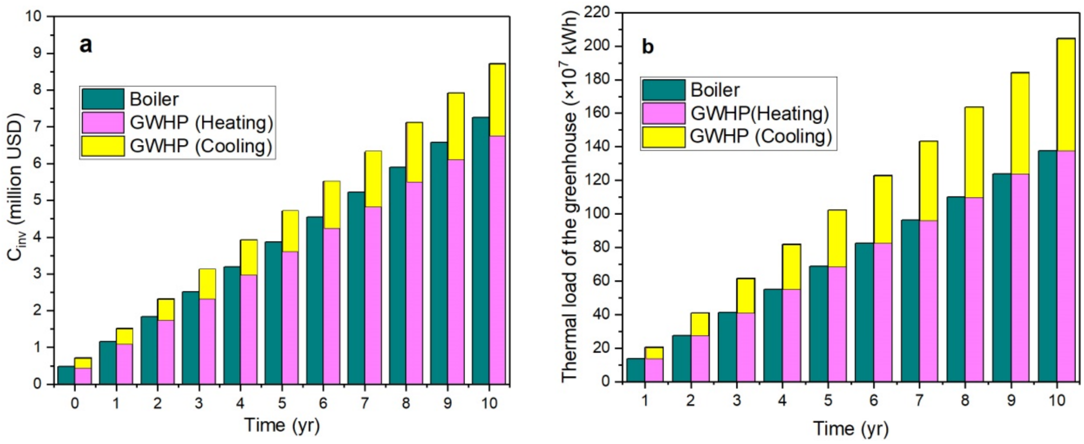

(a) The system investment which consists of capital costs and annual operating costs

(b) The operation benefits for both the boiler and GWHP system

Fig. 16 The comparison of the estimated economic performance for both the boiler and Groundwater Heat Pump system

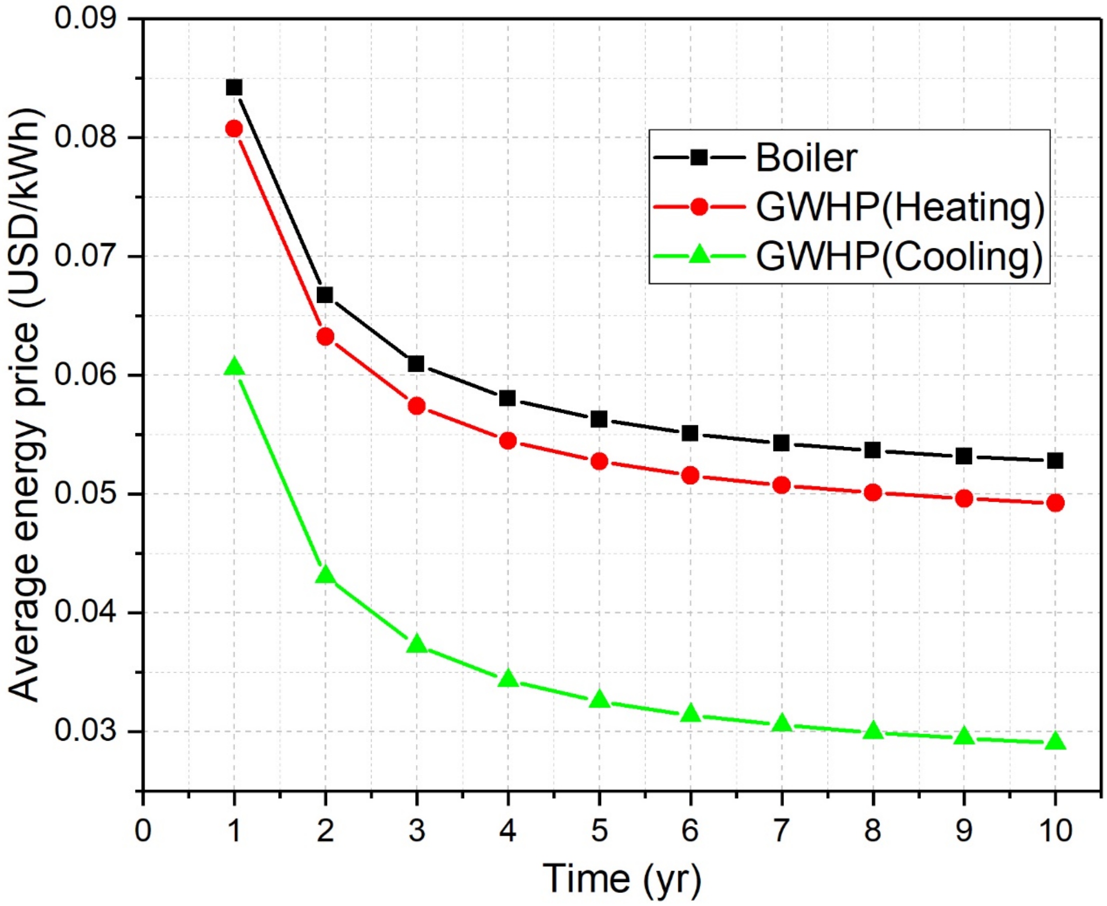

Fig. 17 The estimated average energy price (AEP) for the boiler and GWHP system over a 10-year period

Table 1 Monthly climatic parameters at Zhongxiang city of Hubei province in 2018 [22]

Month	Rainfall	Mean wind	Air temperature	Relative humidity	Sunshine
	mm	(m/s)	(m)	%	h
January	70.2	3.1	1.5	82.9	82.6
February	34.9	3.1	6.2	70	141.3
March	82.2	3.3	13.6	78	145.2
April	84.7	3.6	19.3	72.53	187.4
May	140.8	3.1	23.3	79.1	132.5
June	94.5	2.7	27.3	75.1	209.3
July	198.7	2.8	29.7	83.2	209.5
August	78.9	2.9	29.7	75.7	265.3
September	54.8	2.6	24.3	74.1	132.4
October	14.5	2.5	18.9	59.7	184.8
November	53.3	3	12.7	75.9	123.5
December	36.4	2.9	5.7	74.1	59.6

Table 2 Components and the specifications of the boiler and the GWHP system

System	Components	Number	Type	Specification
Boiler system	Combustion chamber	2	SIL25-1.25-AII	Evaporation capacity: 25 t/h, Working pressure: 1.25MPa, Vapor temperature: 194℃, Water-supply temperature: 104℃, Water volume: 27m3, Efficiency:: 82.8%
	Dust collector	2		Desulphurization: 99%, Dust removal: 99%, Resistance loss: 700, Liquid-to-gas ratio: 1:1, Temperature: <200℃
	Draught fan	2	GY20-15	Rotation speed: 1450 r/min, Flow rate: 62888-92540m^3/h,

				Rated power: 110kW
	Water circulation pump	1	KQL 150/315-30/4	Flow rate：200 m^3/h，H=32m, Power supply：30 kW
	Blower fan	2	GG20-15 55kW	Rotation speed： 1450 r/min, Flow rate: 35000-62000m^3/h, Rated power: 55kW
GWHP system	Heat pump	3	40STD-T-3486W-D4	Power supply: 380V, Heating/cooling Capacity: 3779 kW /3706 kW Refrigerant: R22, 624 kg Energy efficiency ratio: 7.0
	Desander	18	RY-RL	Flow rate: 80m^3/h Pipe diameter: 100 mm
	Water circulation pump (to the greenhouse)	3	TD-300-55/4SWHCJ	Flow rate: 900 m^3/h H=55 m Rated power: 200 kW
	Water pump (to wells)	3		Flow rate:120 m^3/h H=14 m Rated power: 60 kW
	Water pump (to heat pumps)	30		Flow rate: 60 m^3/h Rated power: 11kW

Table 3 Monitoring setup of groundwater heat pump system

Monitoring parameters	Monitoring points	Measuring interval	Symbol	Unit
Fluid temperature into injection wells	1	1 h	T_f	℃
Fluid temperature out	1	1 h	T_f	℃

from production wells				
Fluid temperature into the greenhouse	1	1 h	T_f	℃
Fluid temperature out from the greenhouse	1	1 h	T_f	℃
Air temperature inside Greenhouse	4	1 h	T_{air}	℃
Circulating fluid flow	2	1 h	W	m^3/h
Power input of WP to wells	4	1 d	Q	kWh
Power input of GWHP units	2	1 d	Q	kWh
Power input for WP to greenhouse	2	1 d	Q	kWh
Power input for WP to wells	2	1 d	Q	kWh

Table 4 The recorded drawdown values and the estimated hydraulic parameters of the aquifer

No.	Pumping drawdown (m)	Observation drawdown (m)	Pumping rate (m^3/h)	Hydraulic conductivity (m/s)	Undisturbed Water level (m)	Water temperature (℃)
1	21.5	9.90	72	1.01×10^{-3}		
2	17.3	6.20	67	1.06×10^{-3}	3.0	17 .0±0.5
3	15.5	5.74	60	1.02×10^{-3}		

Table 5 Geochemical analysis of the water samples collected from the drilling well

Parameters	PH	Electric conductivity	Fe^{2+}	Mn^{2+}	Ca^{2+}	Mg^{2+}	Sulfide

		μS/cm	mg/L	mg/L	mg/L	mg/L	mg/L
Value	7.09	973	0.84	1.38	68.50	20.3	0.007

Table 6 The coal consumption of the boiler heating in the heating seasons of the greenhouse from October 16th, 2016 till April 17th, 2017

Time	Coal (Ton)	Heating area (m^2)	Unit heat release (MJ/kg)	Total energy (10^6MJ)	Unit area heat release (MJ/10^6 m^2)
Oct-16	291	175, 400	29.31	8.53	48.62
Nov-16	775	175, 400	29.31	22.71	129.49
Dec-16	1, 439	175, 400	29.31	42.17	240.43
Jan-17	1, 893	175, 400	29.31	55.48	316.28
Feb-17	210	175, 400	29.31	6.15	35.09
Mar-17	538	175, 400	29.31	15.77	89.89
Apr-17	196	175, 400	29.31	5.74	32.75

Table 7 The operating records of the groundwater heat pump (GWHP) system for both heating and cooling

Operating records		Operating conditions	
		Cooling	Heating
Energy consumption	Well pumping (kW)	199-330	199-330
	Heat pumps (kW)	528-1, 584	720-2, 160
	Well injection (kW)	200-600	200-600
	Greenhouse water circulation (kW)	60	60
Fluid flow rate	Well (m^3/h)	540-1, 620	540-1, 620

	Greenhouse (m^3/h)	700-2, 100	700-2, 100
Working hours	System operation (h)	52	169

Table 8 Comparison of the capital costs of both the boiler and groundwater heat pump system

Boiler system			GWHP system		
Components	No.	Price (USD)	Components	No.	Price (USD)
Water tank +Combustion chamber	2+2	224, 510	Heat pump	3	164, 450
Dust collector	2	1, 716	Desander	18	143
Draught fan	2	3, 289	Greenhouse water pumps	3	3, 289
Blower fan	2	3, 475	Well injection pump	3	2, 860
Water circulation pump	1	143	Well pumping pump	30	172
Installation	-	14, 300	Well drilling	60	3, 289
Total		480, 423			716, 859

Table 9 Comparison of the operating costs for both the boiler system in 2016/2017 and groundwater heat pump (GWHP) system in 2018/2019

Operating costs	System		
	Boiler	GWHP	
	Heating	Heating	Cooling
$Q_{e,B/C}$ (kWh)	1, 464, 600	6, 144, 502	1, 185, 184
P_e (USD/kWh)	0.104	0.104	0.104
Q_t (ton)	5, 342	-	-

P_{coal} (USD/ton)	100.1	-	-
C_{main}(USD)	7, 150	7, 150	
Total (USD/yr)	694, 202	769, 437	

Table 10 The estimated annual system investments and thermal loads of the boiler system and the GWHP system

Economic factor	System			
	Boiler	GWHP		
		Heating	Cooling	Total
C_{cap} (USD)	480, 432	481, 825	235, 034	716, 859
C_{oper} (USD/yr)	677, 771	628, 923	171, 309	800, 232
Q_s (kWh/yr)	13, 754, 341	13, 754, 341	6, 709, 352	20, 463, 693

Declaration of Interest Statement

We declare that we have no financial and personal relationships with other people or organizations that can inappropriately influence our work, there is no professional or other personal interest of any nature or kind in any product, service and/or company that could be construed as influencing the position presented in, or the review of, the manuscript entitled **"Thermo-economic comparison of coal-fired boiler-based and groundwater-heat-pump based heating and cooling solution – A Case study on a greenhouse in Hubei, China"**.

Sincerely yours,

Jin Luo, Wei Xue, Haibing Shao